Translational Stroke Research (2021) 12:331–346
https://doi.org/10.1007/s12975-020-00826-9

ORIGINAL ARTICLE

Obesity Drives Delayed Infarct Expansion, Inflammation, and Distinct Gene Networks in a Mouse Stroke Model

Todd C. Peterson[1,2] · Kendra J. Lechtenberg[1] · Brian D. Piening[3,4] · Tawaun A. Lucas[1] · Eric Wei[3] · Hassan Chaib[3] · Alexa K. Dowdell[4] · Michael Snyder[3] · Marion S. Buckwalter[1,5,6]

Received: 30 January 2020 / Revised: 11 May 2020 / Accepted: 3 June 2020 / Published online: 25 June 2020

Abstract

Obesity is associated with chronic peripheral inflammation, is a risk factor for stroke, and causes increased infarct sizes. To characterize how obesity increases infarct size, we fed a high-fat diet to wild-type C57BL/6J mice for either 6 weeks or 15 weeks and then induced distal middle cerebral artery strokes. We found that infarct expansion happened late after stroke. There were no differences in cortical neuroinflammation (astrogliosis, microgliosis, or pro-inflammatory cytokines) either prior to or 10 h after stroke, and also no differences in stroke size at 10 h. However, by 3 days after stroke, animals fed a high-fat diet had a dramatic increase in microgliosis and astrogliosis that was associated with larger strokes and worsened functional recovery. RNA sequencing revealed a dramatic increase in inflammatory genes in the high-fat diet-fed animals 3 days after stroke that were not present prior to stroke. Genetic pathways unique to diet-induced obesity were primarily related to adaptive immunity, extracellular matrix components, cell migration, and vasculogenesis. The late appearance of neuroinflammation and infarct expansion indicates that there may be a therapeutic window between 10 and 36 h after stroke where inflammation and obesity-specific transcriptional programs could be targeted to improve outcomes in people with obesity and stroke.

Keywords Stroke · Obesity · Neuroinflammation · Macrophages · Infarct expansion

Introduction

Neuroinflammation after stroke causes bystander death of neurons that leads to infarct expansion [1–3]. Given that neuroinflammation is instigated by stroke and lasts for days afterward, it is an attractive therapeutic target. However, much of this work has been done in otherwise normal animals. To design therapies for people with stroke, it is important to understand how the physiologic state induced by common comorbid conditions influences the neuroinflammatory response to stroke. Obesity is highly relevant because it induces chronic low-grade peripheral inflammation. Over one third of the US population is obese (body mass index (BMI) > 30), and an additional third is overweight (BMI 25–30) [4, 5]. In addition, people who are overweight are 22% more likely to have a stroke, while those who are obese are 64% more likely [6]. It is therefore critical to study the effects of obesity on neuroinflammation and stroke.

Outside the brain, diet-induced obesity polarizes immune cells towards a more pro-inflammatory state. In adipose tissue, monocyte chemoattractant protein 1 (MCP-1) and other cytokines released by adipocytes recruit both

Electronic supplementary material The online version of this article (https://doi.org/10.1007/s12975-020-00826-9) contains supplementary material, which is available to authorized users.

✉ Marion S. Buckwalter
marion.buckwalter@stanford.edu

[1] Department of Neurology and Neurological Sciences, Stanford School of Medicine, Palo Alto, CA, USA

[2] Department of Psychology, University of North Carolina Wilmington, Wilmington, NC, USA

[3] Department of Genetics, Stanford School of Medicine, Palo Alto, CA, USA

[4] Earle A. Chiles Research Institute, Providence Portland Medical Center, Portland, OR, USA

[5] Department of Neurosurgery, Stanford School of Medicine, Palo Alto, CA, USA

[6] Department of Neurology and Neurological Sciences and Department of Neurosurgery, Stanford University, P209 MSLS Building, 1201 Welch Road, Stanford, CA 94305, USA

blood and tissue monocytes and macrophages to infiltrate adipose tissue, where they adopt a more pro-inflammatory state and recruit and polarize T lymphocytes towards a pro-inflammatory Th1 state [7–10]. Adipose tissue then acts as a pro-inflammatory organ and drives a concomitant increase in pro-inflammatory cytokines in the blood [11–14].

Diet-induced obesity also increases blood-brain barrier permeability, leading to neuroinflammation in specific areas of the brain. After at least 6 weeks of high-fat diet, there are reduced tight junction proteins in brain vascular endothelial cells [15] and resultant increases in the infiltration of macromolecules into the hippocampus and hypothalamus [16, 17]. This permeability results in chronic, low-grade inflammation in these subcortical regions, manifested by increased pro-inflammatory cytokine levels, glial cell activation, and neuronal dysfunction [18–23].

When a stroke occurs in the pro-inflammatory context of obesity or diabetes, infarct size is typically larger [24–32]. Only a small number of studies have examined the neuroinflammatory response after stroke in diet-induced obesity models, and these demonstrated increases in canonical pro-inflammatory cytokines, tumor necrosis factor (TNF) and interleukin-6 (IL-6) [28], and a qualitative increase in microgliosis [27]. Following longer high-fat diet exposure prior to stroke, Maysami et al. [33] reported blood-brain barrier injury, increased pro-inflammatory cytokine expression, and higher neutrophil numbers 1 day after stroke.

These studies raised the possibility that the molecular signature of the neuroinflammatory response to stroke in obese animals might be different than that in non-obese animals, and further that this might reflect a unique state that would require a different therapeutic approach. It has not been known whether pre-existing changes in the brain in obesity are the primary driver of these worsened outcomes or, alternatively, whether increased inflammation in the peripheral immune system drives at least some of the increased neuroinflammation after a stroke has occurred. The latter would mean that there is potentially a therapeutic window after stroke during which harmful neuroinflammation could be abrogated.

To address these questions, we used a standard paradigm to produce diet-induced obesity [34]. We fed wild-type C57BL/6J mice high-fat or control diet for 6 weeks or 15 weeks prior to stroke and examined neuroinflammation before and at 10 hours and 3 days after stroke. We then assessed infarct size and the effect on motor recovery. To mimic the experience of patients in a hospital, all mice were placed on control diet after stroke. Finally, we performed RNA sequencing on cortical samples from naive and stroked mice following normal or high-fat diet and determined transcriptional changes that occurred in the brain from diet alone and after stroke.

Materials and Methods

Experimental Animals

Animals were utilized according to protocols approved by the Stanford Institutional Animal Care and Use Committee and the NIH Guide for Care and Use of Animals. One hundred and forty-five 10–12-week-old female C57BL/6J mice (https://www.jax.org/strain/000664) were used. Animals were fed a 60% kcal fat diet (no. D12492; Research Diets, Inc., New Brunswick, NJ) or a *normal* 18% kcal fat diet (no. 2018SX; Harlan Laboratories, Indianapolis, IN) for 6 weeks or 15 weeks. To measure glucose tolerance, animals fasted for 24 h, and then blood glucose (tail vein) was measured (FreeStyle Freedom Lite (70827); Medline Industries, Inc., Northfield, IL) prior to and 5, 15, 30, 60, 90, 120, and 180 min after a bolus i.p. injection of 2 g of glucose/kg [35]. All of the experiments were completed in compliance with the ARRIVE guidelines for how to report animal experiments.

Stroke Models

Animals were anesthetized with 2% isoflurane in 100% oxygen and maintained at 37 °C. For the 10- and 72-hour (3 day) sacrifice time points, animals underwent distal middle cerebral artery occlusion (dMCAO), which creates a primarily cortical infarct [36, 37]. Briefly, an incision was made along the animals' skull, and the temporalis muscle transected to expose the middle cerebral artery through the skull. A craniotomy was then drilled, and the artery cauterized. The muscle and skin were replaced, and after closure, the animals received cefazolin (25 mg/kg s.c., no. 89149-888, VWR) and buprenorphine SR (1 mg/kg s.c.; ZooPharm, Windsor, CO). The dMCAO model provides a physiologically relevant model of ischemia, but no long-term functional deficits are incurred.

Photothrombotic stroke was targeted over the motor cortex to provide contralateral motor forelimb deficits and was only utilized for behavioral experiments to measure functional recovery. Mice were injected intraperitoneally with 100 mg/kg Rose Bengal (no. 330000 5G, Sigma) in sterile saline, placed in a stereotactic frame, and a Metal Halide Fiber optic light (no. 56371, Edmundonoptics) focused to a 1 mm diameter with a × 10 microscope objective was placed directly over the right motor cortex (− 0.5 mm posterior, + 1.75 mm lateral to bregma) for 15 min.

Immunohistochemistry

Animals were perfused with 10 U/mL heparin in 0.9% NaCl, and brains were drop fixed in 4% paraformaldehyde in phosphate buffer overnight, then sunk in 30% sucrose in PBS. Forty-micrometer-thick coronal brain sections were sectioned

using a freezing sliding microtome (Microm HM430), collected sequentially in 16 tubes, and then stored in cryoprotective medium (30% glycerin, 30% ethylene glycol, and 40% 0.5 M sodium phosphate buffer) at 20 °C until processed. Standard immunohistochemistry procedures were used to stain free floating sections using antibodies as described in Supplementary Table 1. For cresyl violet counterstaining, mounted sections were dehydrated and submerged in cresyl violet for 5 min.

Quantification Procedures

To calculate stroke size, we immunostained ten coronal sections that spanned the infarct and were spaced exactly 320 μm apart with NeuN, then counterstained with cresyl violet. We imaged with a PathScan Enabler IV (Meyer Instruments, Houston, TX) and traced the infarct and hemisphere volumes with ImageJ software (version 1.51c, 2017). For dMCAO, the percent of infarcted hemisphere (infarcted area (contralateral hemisphere area / (ipsilateral area without infarcted area + infarcted area)) / contralateral hemisphere × 100) was used to quantify infarct core, which controls for edema that often occurs in the side ipsilateral to the stroke [38]. For photothrombotic stroke, the direct volume was used to measure the infarct volume as this model has very little associated edema at 29 days.

To image microgliosis and astrogliosis, we immunostained five sections spaced 640 μm apart for CD68 and glial fibrillary acidic protein (GFAP), respectively. Two × 40 images were captured in the peri-infarct cortex, one medial to and one lateral to the stroke core, each one view field distance (543 μm) away from the stroke border. In ImageJ, images were set to an 8-bit color (black and white) and blindly quantified at a uniform threshold that encompassed area covered (density) of the soma and processes of each cell type.

To count Iba1-expressing cells, two z-stacks were taken in the peri-infarct area (similar to above) at × 40 magnification on three tissue sections centered around the infarct and 640 μm apart. Iba1+ cells were quantified using ImageJ software. To quantify Iba1 fluorescence area, images were converted to 8-bit and thresholded using the default mode in the ImageJ software.

Real-Time Quantitative PCR

To obtain RNA, mice were fed control diet or high-fat diet for 6 weeks, then sacrificed either prior to (naïve) or 10 h or 72 h (3 days) after stroke. Strokes are visible by eye at this time point, and cortical tissue was dissected that contained the stroke core and 1–2 mm of surrounding penumbral tissue. Cortical peri-infarct tissue was flash frozen, RNA was extracted (TRIzol, no. 15596-026, Invitrogen) and converted to complementary DNA (cDNA) (High-Capacity cDNA RT kit, no. 4368814, Applied Bioscience). Quantitative PCR was used to measure gene expression changes. Reactions were performed in a 384-well plate with SYBR Green (no. 204143, Qiagen) and run on a QuantStudio 6 Flex (no. 4484642, Thermo Fisher Scientific) qPCR machine. Primers are listed in Supplementary Table 2. Results were normalized to *Hprt* using the ΔΔCt method.

Behavioral Assessments

To measure functional recovery following photothrombotic stroke to the motor cortex, we utilized the tapered beam, foot fault, and rotating beam tasks [39–42]. For each task, there was one habituation day and two pre-training days prior to photothrombotic stroke. Animals were also tested on days 1, 3, 7, 14, and 28 following photothrombotic stroke. For tapered beam, the number of contralateral forelimb faults was recorded as they progressed down the beam, during four trials each day. For foot fault, animals were allowed to explore freely for 2 min and the number of contralateral forelimb faults was recorded. As the rotarod is often used to measure gross motor deficits that are not present in this model [43], we instead used the rotating beam [42], animals were placed on a rotating beam (6 rpm) which they transverse longitudinally, and the distance covered prior to falling was recorded, for four trials each day.

RNA Sequencing

RNA library preparation was performed using an Agilent Bravo automated liquid handling platform using Illumina TruSeq Stranded Total RNA HT reagents. Final libraries were assessed for quantity and quality on a Fragment Analyzer instrument (Advanced Analytical). Multiplexed paired-end libraries were pooled and sequenced on an Illumina HiSeq 4000 instrument at 300 cycles, generating, on average, 20–30 million reads per library sample. Following sequencing, reads were trimmed of adapter sequences using *Trim Galore!* and mapped to the mm9 mouse reference genome using the STAR aligner. Read counting was performed at the gene level using the *featureCounts* function in HTSeq. Normalization and differential expression testing were carried out using the edgeR package in R/Bioconductor [44, 45]. Genes whose counts did not average to 10 across all samples were filtered out as low/non-expressing. Differential expression was then carried out, and top genes were selected based on false discovery rate (FDR), and adjusted *p* values calculated using the Benjamin-Hochberg (BH) method of correction. We examined Gene Ontology pathways with Cytoscape [46], using automatic weighting, indicating to find "zero" top related genes in the analysis [47]. Pathway analysis was conducted for association with Gene Ontology categories using the GeneMANIA

package [47] in Cytoscape [46] after filtering using DESeq2 (version 3.9) [48].

Rigor and Statistical Analyses

For all experiments, animals were randomized and concealed, and experimenters blinded. The only animals excluded from analysis were those that did not survive until the final endpoint after photothrombotic stroke, and this is noted in the results. GraphPad Prism software (version 8) and R [49] were used for graphing and statistical analyses. The difference of means was assessed by the two-tailed Student's t test for 2 groups and a two-way ANOVA and Sidak post hoc analysis for > 3 groups. Results are presented as means ± 95% confidence intervals (CIs). For functional recovery assays, linear mixed-effects models were utilized with the lme4 package in R statistical package [50], as it shows greater sensitivity than a repeated-measures ANOVA [51]. In the model, subjects (i.e., mice) were specified as a random factor to tolerate the unequal group sizes by day due to mortality, and then ANOVA tests were used for differences between the models. To assess the significance of the survival curve, we used a Kaplan-Meier analysis.

Data Availability

The RNA-seq datasets are uploaded to the NCBI Gene Expression Omnibus (GEO) (https://www.ncbi.nlm.nih.gov/geo/query/acc.cgi?acc=GSE104882) with the number GSE104882. The data is also available on our laboratory website in an easily accessible format (buckwalterlab.shinyapps.io/SixWeekHighFatDietStrokeData/).

Results

High-Fat Diet Causes Weight Gain, Glucose Intolerance, and Larger Infarct Size

To generate diet-induced obesity, we fed C57BL/6J mice a high-fat diet for either 6 weeks or 15 weeks (Supplementary Fig. 1) and examined weight and glucose tolerance. Animals fed a high-fat diet for 6 weeks were 19.8% heavier, while animals fed a high-fat diet for 15 weeks were 53.9% heavier than control diet–fed animals (Supplementary Fig. 1B). Weight gain was similar to that reported [52, 53] and consistent between cohorts (data not shown). We verified the expected glucose intolerance [54, 55] and found high-fat diet-fed animals were indeed not diabetic but did exhibit significantly ($p < 0.001$) impaired glucose tolerance (Supplementary Fig. 1C).

To assess infarct volume, we performed dMCAO strokes. This permanent ischemia model has the advantage that there is a sharp delineation between the infarct and uninjured tissue and relatively low variability [37], allowing precise measurement of the inflammatory response relative to the stroke border. We induced dMCAO following either 6 weeks or 15 weeks of high-fat diet and measured infarct sizes at 3 days (Fig. 1a). Animals fed high-fat diet for either 6 weeks or 15 weeks had significantly larger infarct volumes, 136.5% larger infarct volume than those on a control diet ($p < 0.05$) after 6 weeks, and 142.9% larger infarct volume ($p < 0.01$) after 15 weeks of high-fat diet. There was no difference in infarct enlargement between the two diet paradigms ($p = 0.896$).

Diet-Induced Obesity Animals Have Worsened Functional Recovery Following Ischemia

The only experimental photothrombotic stroke was used to assess functional recovery. This model, unlike dMCAO (which targets the sensory cortex), produces a motor deficit that persists after stroke [3, 56]. We used a photothrombotic stroke model to target the motor cortex after 6 weeks of control or high-fat diet. There was no effect of either diet or weight on behavioral measures prior to stroke (Supplementary Fig. 2 and data not shown for the gridwalk foot fault task). We measured recovery over the next 28 days. Interestingly, we observed increased fatality in the high-fat diet-fed animals (Fig. 1b), which was not observed with the dMCAO strokes in either diet group (data not shown).

We measured recovery of the limb contralateral to the stroke 1, 3, 7, 14, and 28 days after stroke and found significantly worse behavioral performance in high-fat diet-fed animals. In a linear mixed-effects model followed by type II ANOVA, the main effect of diet and day after stroke significantly predicted the number of errors during the tapered beam task ($p = 0.018$ and $p < 0.0001$, respectively), with mice fed high-fat diet displaying significantly more errors on the task (Fig. 1c). Additionally, animals fed high-fat diet performed significantly worse on the rotating beam task (Fig. 1d). Both diet and day significantly predicted distance traveled in a linear mixed-effects model with the high-fat diet-fed animals performing significantly worse ($p < 0.0001$). There were no significant differences between groups in a gridwalk foot fault task ($p = 0.473$, data not shown).

Following the behavioral assessments, on day 29, we perfused the animals and conducted an infarct analysis of the photothrombotic stroke core. Even after excluding the mice that died during the experiment, animals fed a high-fat diet had significantly larger infarct volumes after photothrombotic stroke than control diet–fed animals ($p < 0.01$, Fig. 1e).

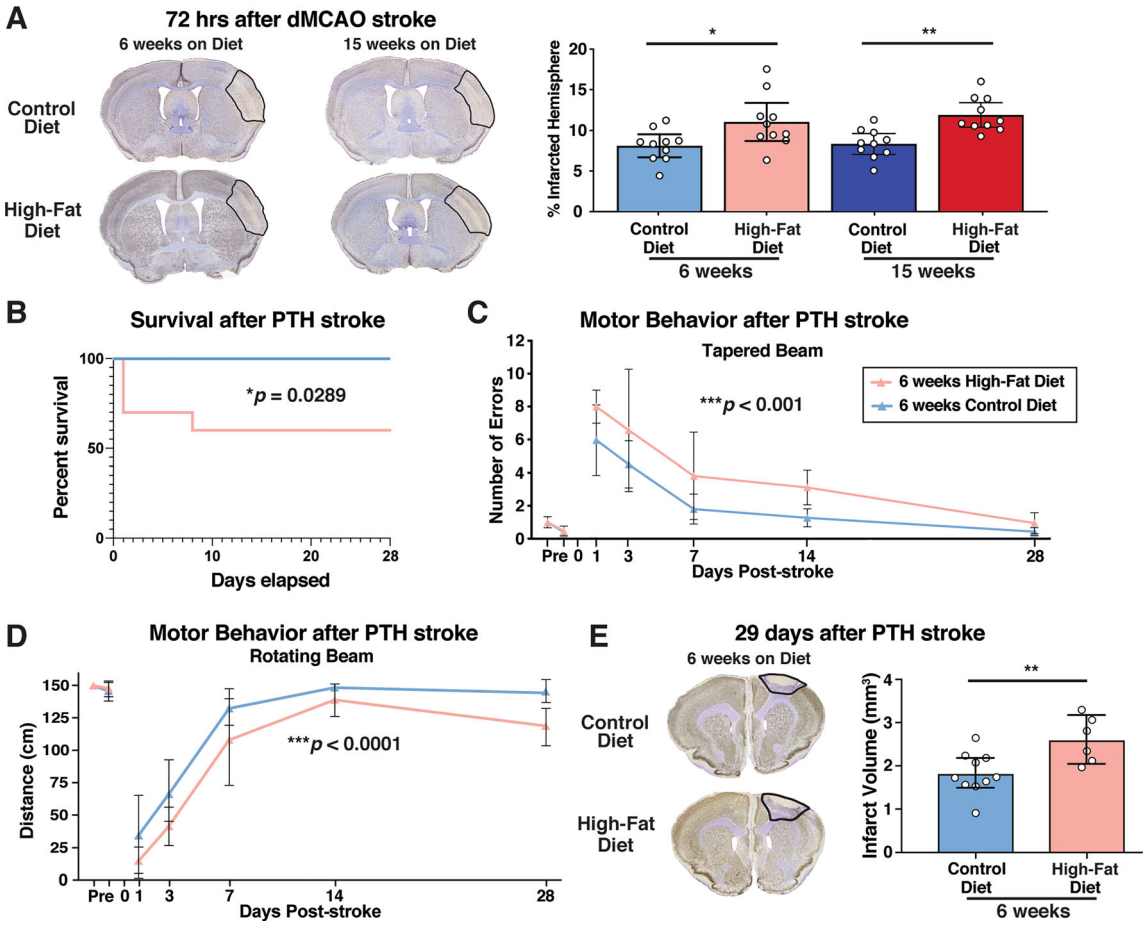

Fig. 1 High-fat diet-fed animals exhibit increased infarct size and are more impaired after stroke than animals on control diet. **a** Representative photomicrographs 3 days after dMCAO stroke, stained with the neuronal marker NeuN and cresyl violet following either 6 weeks or 15 weeks of control diet or high-fat diet, and quantification of infarct size (as percent infarcted area) showed that in both conditions, animals fed high-fat diet had larger infarct sizes than their control diet–fed counterparts at 3 days after stroke. **b**–**e** An additional group of animals was given photothrombotic stroke in the motor cortex to examine motor recovery. **b** Survival curve demonstrating a significant mortality rate of 40% in the high-fat diet-fed animals and a mortality rate of 0% in the control diet–fed animals ($n = 10$/group). Performance on both **c** tapered beam and **d** rotating beam tasks (bottom) is identical pre-stroke but worse in animals fed high-fat diet for at least 28 days after stroke (linear mixed-effects models, compared statistically with ANOVA: $F = 35.27$ ($p < 0.001$) for tapered beam and $F = 103.21$ ($p < 0.0001$) for rotating beam). Linear-mixed effects model demonstrates significant differences between diet groups in both tasks following stroke. **e** Representative photomicrographs 29 days after photothrombotic stroke, stained with the neuronal marker NeuN and counterstained with cresyl violet (top), and quantification of absolute infarct volume (bottom) showed that animals fed 6 weeks of high-fat diet had significantly larger infarct sizes than their control diet–fed counterparts at 29 days after photothrombotic stroke. Error bars ± 95% CI; $*p < 0.05$, $**p < 0.01$, $***p < 0.001$, $****p < 0.0001$

Diet-Induced Obesity Elicits Dramatic Increases in Stroke-Induced Neuroinflammation

We next analyzed whether the neuroinflammation is elicited by stroke, measured by the area covered by each cell type, which was increased by diet-induced obesity. Immunohistochemistry for GFAP was used to assess astrogliosis in the peri-stroke cortex 3 days after stroke, when the response is at peak. Animals fed a high-fat diet for either 6 weeks or 15 weeks had significantly more GFAP immunostaining, approximately a 150% increase in percent area covered over control diet–fed animals (Fig. 2a, b). CD68 immunostaining was used to assess activated microglia and monocyte-derived macrophages that come from the bloodstream, as both are important for phagocytosis of the stroke core but also can propagate harmful immune responses. Differences in CD68 immunostaining were even greater. Animals fed high-fat diet for 6 weeks had 202% more area covered by staining for CD68, while the animals fed a high-fat diet for 15 weeks had a 159% larger response than controls (Fig. 2c, d). Because we found no differences between animals on 6 and 15 weeks of high-fat diet with either neuroinflammation measure or infarct size, we conducted the remainder of experiments on animals fed high-fat diet for 6 weeks.

To investigate the CD68 immunostaining differences, we stained for Iba1 to capture all microglia and monocyte-derived

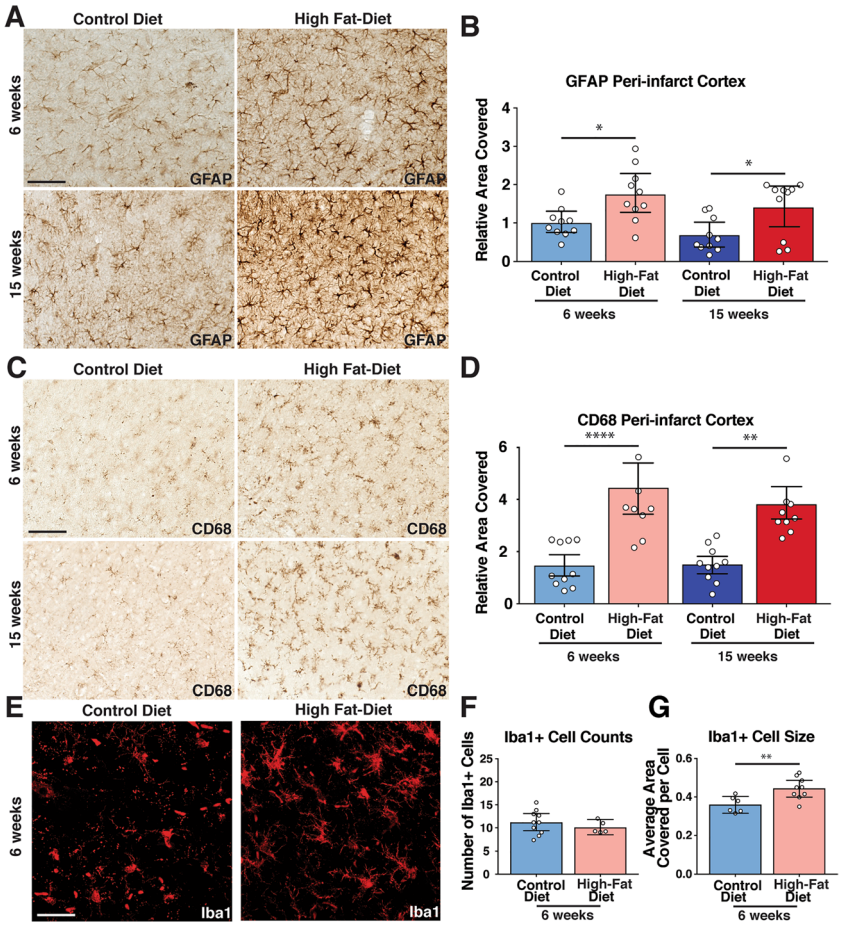

Fig. 2 Increased activation of astrocytes and microglia 3 days after stroke in high-fat diet-fed animals. **a** Representative photomicrographs of GFAP-immunostained cortex following either 6 weeks or 15 weeks of high-fat diet. **b** Quantification of percent area covered by GFAP immunostaining. **c** Representative photomicrographs of CD68-immunostained cortex following either 6 weeks or 15 weeks of high-fat diet. **d** Quantification of percent area covered by CD68 immunostaining. **e** Confocal z-stacks of Iba1-immunostained cells in the peri-infarct cortex. **f** Quantification of Iba1+ cell numbers in the peri-infarct cortex. **g** Quantification of average area covered per Iba1+ cell. Scale bars 100 μm; error bars ± 95% CI; $*p < 0.05$, $**p < 0.01$, $****p < 0.0001$

macrophages (Fig. 2e). There were no significant differences between the numbers of Iba1+ cells in the peri-infarct area (Fig. 2f), but the average area covered per cell was significantly larger in animals fed a high-fat diet for 6 weeks prior to stroke (Fig. 2g). Thus, the microgliosis induced by high-fat diet is due to a change in cell morphology rather than increased number.

Diet-Induced Obesity Does Not Induce Neuroinflammation in the Uninjured Brain

Next, we asked whether the increased neuroinflammation at 3 days was due to diet-induced neuroinflammation prior to stroke. Interestingly, there were no differences in cell morphology or the percent area covered by GFAP+ astrocytes or CD68+ macrophages (Fig. 3a), indicating no gross change in neuroinflammation from diet alone.

Animals Fed High-Fat Diet Do Not Have Larger Infarct Volumes or Increased Neuroinflammation 10 Hours After Stroke

Given that there was no prominent neuroinflammation before stroke, we evaluated it shortly after stroke to determine if there might be a therapeutic window where the brain is not yet affected by peripheral inflammation, choosing 10 hours as it is a clinically tractable window. We fed mice a high-fat or control diet for 6 weeks and sacrificed them 10 hours after stroke. At this 10-hour time point, there was no significant infarct volume difference (Fig. 3b). Notably, similar to the naïve (pre-stroke) mice, there was no difference between the groups in either astrogliosis or microgliosis (Fig. 3c) 10 hours after stroke. Thus, although there is clearly increased inflammation measured by immunohistochemistry by 3 days after stroke, both stroke expansion and the increased neuroinflammation occur between 10 hours and 3 days after stroke.

Animals with Diet-Induced Obesity Have Increased Pro-inflammatory and Chemoattractant Gene Expression at 3 Days, but Not Prior to or at 10 Hours After Stroke

We next performed qPCR for neuroinflammatory genes to better characterize the inflammatory changes and determine whether transcriptional differences precede immunohistochemical changes. We evaluated cortical tissue that contained the infarct and peri-infarct cortex (or location-matched cortical tissue in mice before stroke). We chose genes a priori that are implicated in

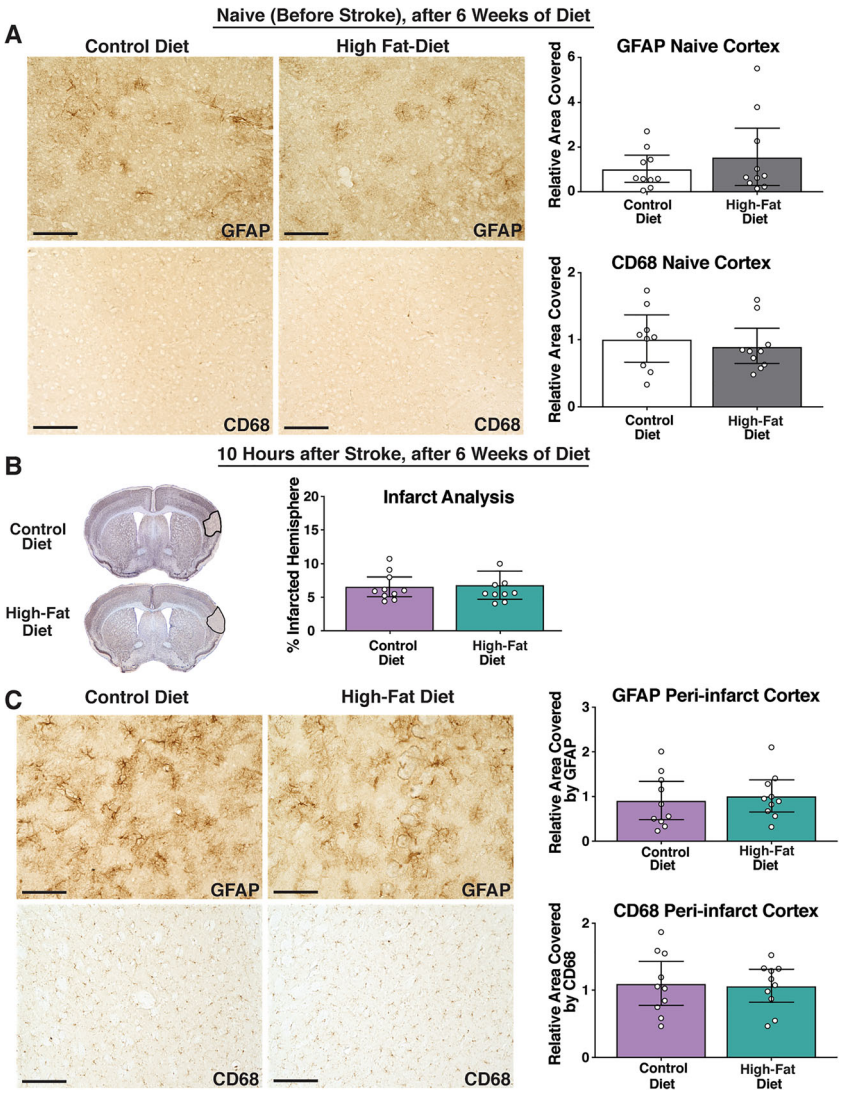

Fig. 3 High-fat diet for 6 weeks does not induce cortical astrogliosis or microgliosis either prior to or 10 h after stroke. **a** Representative photomicrographs and quantification of immunohistochemistry for GFAP and CD68 to measure astrogliosis and microgliosis, respectively, in cortical regions of animals fed 6 weeks of high-fat diet and control diet. **b** Infarct analysis 10 hours after dMCAO stroke in animals fed control or fed high-fat diet for 6 weeks prior to stroke. Representative photomicrographs, stained with the neuronal marker NeuN and counterstained with cresyl violet (left), and quantification of infarct size (percent infarcted area). **c** Representative photomicrographs and quantification of immunohistochemistry for GFAP and CD68 to measure astrogliosis and microgliosis, respectively, in the peri-infarct cortex of animals that were fed 6 weeks of high-fat diet and control diet and then sacrificed 10 h after stroke. Scale bars 100 μm; error bars ± 95% CI

peripheral inflammation following obesity or in the peri-infarct area following stroke. In high-fat diet-fed animals, 3 days after stroke, there was increased expression of the pro-inflammatory genes Nos1, Nfkb, Tnf, and Ccl2/MCP-1 (Fig. 4a–d) and the cell adhesion molecules Vcam1 and Icam1 (Fig. 4e, f). As with our immunohistochemical measures of neuroinflammation, there were no significant differences in any of these genes between the diet groups either prior to or 10 h after stroke. Thus, qPCR for candidate genes confirmed that the neuroinflammation induced by high-fat diet appears in the brain subsequent to the 10-h time point after stroke.

High-Fat Diet Exerted Few Changes on Cortical Gene Transcription Before Stroke

To delve more deeply into transcriptional changes induced by high-fat diet, we performed RNA-seq on mice fed 6 weeks of control or high-fat diet prior to stroke (*naïve* mice). In agreement with immunohistochemistry results, there were minimal differences between high-fat diet-fed and control diet–fed animals (Fig. 5a). Comparing cortical RNA from mice on control versus high-fat diet, only 13 genes were significantly ($p < 0.01$, $\log_2$ fold change, FDR < 0.01) different (Supplementary Table 3). Eight were upregulated transthyretin, prolactin receptor, a mitochondrial tRNA synthetase, two predicted genes, a microRNA, and two ribosomal genes. Calpain 11, Aim-1-like, and the proto-oncogene JunB were among the five downregulated genes. There were no significant Gene Ontology (GO) pathways represented by these gene changes, and none were directly related to inflammatory pathways. This is consistent with only minimal transcriptional changes in the cortex.

Genes Changed by High-Fat Diet After Stroke Are Primarily Pro-inflammatory

We next compared gene expression 3 days after dMCAO stroke (Fig. 5b) in infarct core and peri-infarct cortex. There were 313

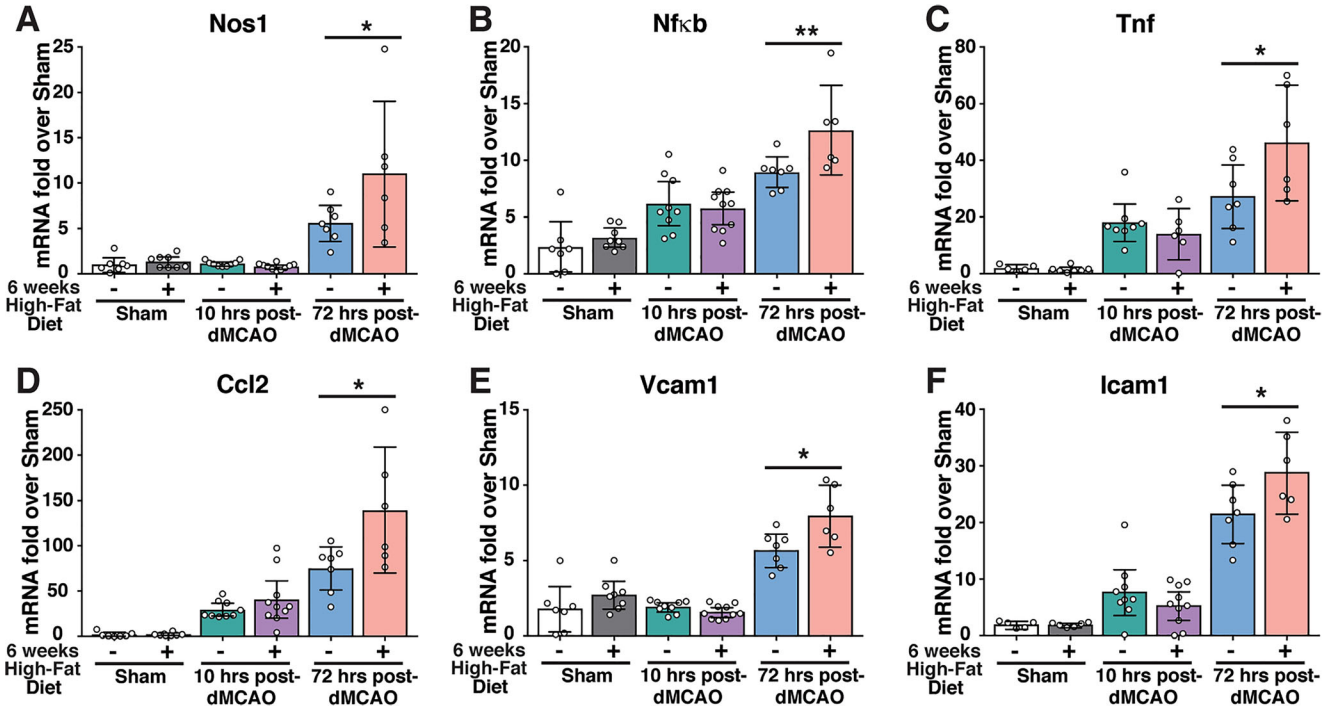

Fig. 4 High-fat diet fed animals had increased gene expression of pro-inflammatory genes at 3 days after stroke, but not pre-stroke or 10 hours after stroke. Groups are 6–10 animals, and gene expression was determined by quantitative real-time PCR. Nos1, nitric oxide synthase 1; Nfκb, nuclear factor kappa B; Tnf, tumor necrosis factor α; Ccl2, C-C motif chemokine ligand 2; Vcam1, vascular cell adhesion molecule 1; Icam1, intercellular adhesion molecule 1; error bars ± 95% CI; $*p < 0.05$, $**p < 0.01$.

genes that were different in high-fat diet-fed than control diet–fed animals. Also mirroring our previous immunohistochemistry and qPCR assessments of neuroinflammation, and in contrast to pre-stroke, the brain transcriptome after stroke was dramatically different in high-fat diet-fed animals versus the control diet–fed animals, with 275 genes significantly upregulated in high-fat diet-fed animals relative to control diet and 38 genes downregulated (Fig. 5b). Thus, the vast majority of changes induced by diet occurred after stroke (Fig. 5c). The top two upregulated genes after stroke were transthyretin and folate receptor 1 (Supplementary Table 4), which were both also upregulated by high-fat diet prior to stroke. The majority of the top 20 downregulated genes had a small log fold change and were predicted genes (Supplementary Table 4).

We performed network visualization with Cytoscape to identify significant relationships among genes changed in this *by diet* comparison of high-fat diet versus control diet after stroke (Fig. 5d). Differentially expressed genes were related to inflammatory responses including IFNβ, defense response, and antigen processing and to injury response and extracellular matrix. GO pathway analysis was consistent with this; the predominant effect of high-fat diet on stroke was to upregulate the immune response (Fig. 5e). The top 20 pathways were related to extracellular matrix remodeling and cell migration (10 pathways), general inflammation or innate immune responses (5 pathways), and antigen processing and adaptive immune responses (5 pathways).

On Either Diet, the Majority of Genes Upregulated by Stroke Are Pro-inflammatory

To ask what was similar versus different between the response to stroke on the two diets, we performed a *by stroke* comparison. We found that there were 1346 genes changed by stroke in mice on control diet, and most of them were upregulated (Fig. 6a). The most downregulated gene in control mice after stroke was transthyretin, which was over 4-fold decreased (Supplementary Table 5). There were nearly twice as many genes that were significantly different after stroke in the high-fat diet-fed mice, 2140 total (Fig. 6b). Many of the genes most upregulated in control diet–fed mice were also among the top 20 most upregulated in the high-fat diet-fed mice and were pro-inflammatory (Supplementary Table 6). Top genes upregulated by stroke in both diets included lipocalin-2, CD5 antigen-like, matrix metallopeptidase 8, Mediterranean fever, platelet selectin, and apolipoprotein C-II.

To further investigate the overlap between the genes changed in stroke in mice on both diets, we segregated them into three groups (Fig. 6c, d), (1) those changed in control diet but not high-fat diet (199 genes), (2) those changed in both diets (1147 genes), and (3) those only altered by stroke in the high-fat diet-fed mice (993 genes). In the 199 changed by stroke in control mice alone, GO pathway analysis revealed only 7 significant GO pathways, most related

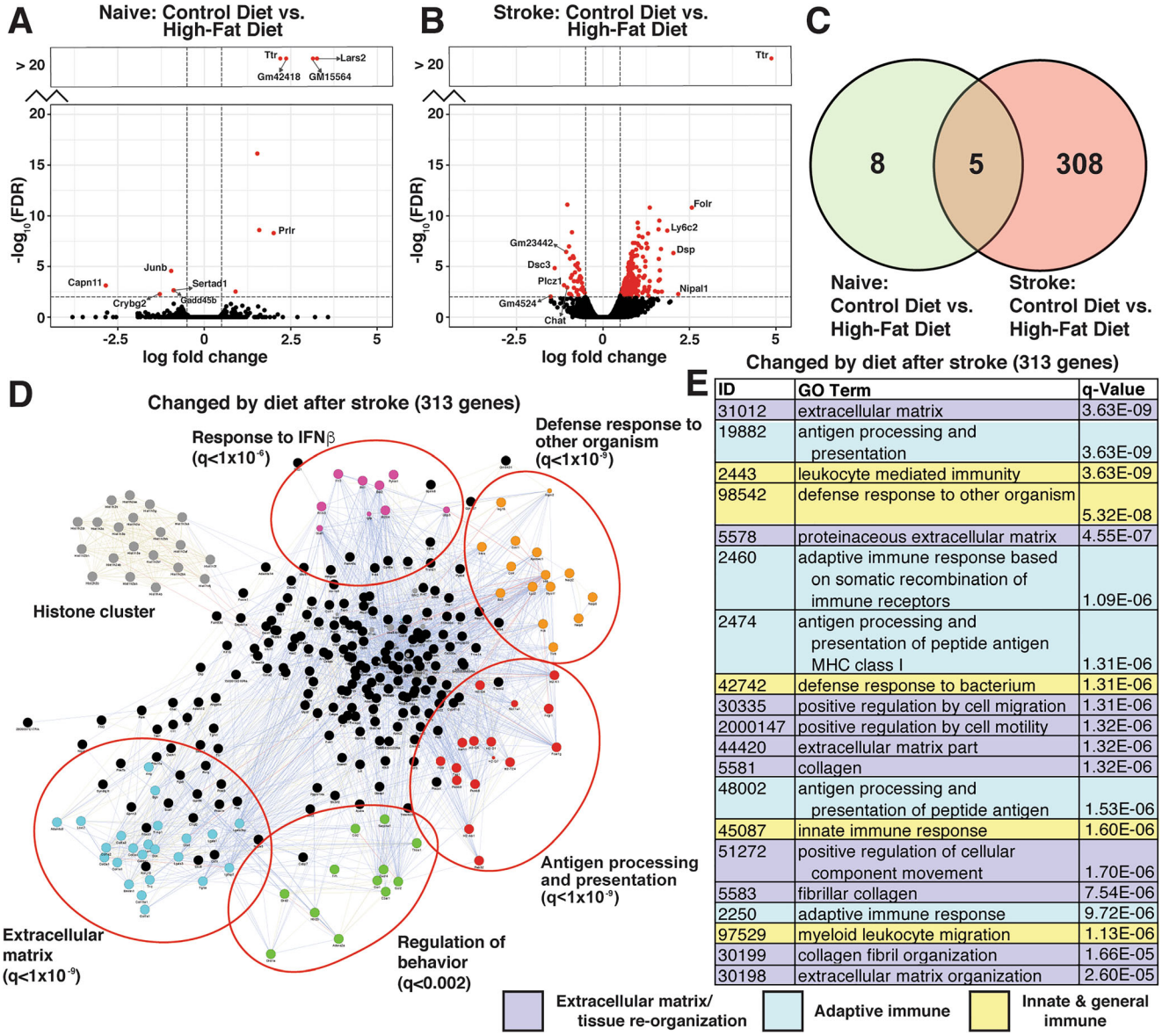

ID	GO Term	q-Value
31012	extracellular matrix	3.63E-09
19882	antigen processing and presentation	3.63E-09
2443	leukocyte mediated immunity	3.63E-09
98542	defense response to other organism	5.32E-08
5578	proteinaceous extracellular matrix	4.55E-07
2460	adaptive immune response based on somatic recombination of immune receptors	1.09E-06
2474	antigen processing and presentation of peptide antigen MHC class I	1.31E-06
42742	defense response to bacterium	1.31E-06
30335	positive regulation by cell migration	1.31E-06
2000147	positive regulation by cell motility	1.32E-06
44420	extracellular matrix part	1.32E-06
5581	collagen	1.32E-06
48002	antigen processing and presentation of peptide antigen	1.53E-06
45087	innate immune response	1.60E-06
51272	positive regulation of cellular component movement	1.70E-06
5583	fibrillar collagen	7.54E-06
2250	adaptive immune response	9.72E-06
97529	myeloid leukocyte migration	1.13E-06
30199	collagen fibril organization	1.66E-05
30198	extracellular matrix organization	2.60E-05

Fig. 5 Differential gene expression in the cortex of high-fat diet-fed compared to control diet–fed animals before (naïve) and 3 days after stroke. **a** Volcano plots indicating levels of differential gene expression for control diet versus high-fat diet in mice fed diet for 6 weeks and before (**a**, naïve) and 3 days after stroke (**b**). The log fold change in gene expression between pairs of conditions is plotted against the false discovery rate (FDR, in negative log base 10). Genes highlighted in red indicate significance at FDR < 0.01. **c** Venn diagram showing the number and overlap in genes significantly different between diets (FDR < 0.01). **d** Cytoscape network plot of significant genes (FDR < 0.01) that differ between high-fat diet and control diet animals after stroke. Node (genes) connections are determined by the GeneMANIA plugin corresponding to known physical interactions (pink), shared protein domains (yellow), and protein co-localization (blue). **e** Top Gene Ontology (GO) pathways altered in high-fat diet-fed mice following stroke. Pathways are color coded into three main biological effects: general and innate inflammation (yellow), extracellular matrix and tissue reorganization (purple), and adaptive immunity (blue)

to muscle, perhaps not surprising given the relatively small number of genes (Fig. 6d). On the other hand, the top twenty GO pathways for the 1147 genes in common were nearly all related to general and innate immune responses. The 993 upregulated by stroke in high-fat diet-fed animals but not control diet animals were associated with additional innate and general inflammatory pathways, and also extracellular matrix remodeling, adaptive immune responses, and angiogenesis/vasculogenesis (Fig. 6d).

A deeper look at the 1147 genes upregulated by stroke in both diets demonstrated that in high-fat diet-fed animals, 1106 are upregulated by stroke, and of these, the vast majority (993) are higher in high-fat diet-fed than control diet–fed mice (Fig. 7a). Comparing the upregulation of classical anti-inflammatory and pro-inflammatory immune genes in this group of genes revealed that although both types of genes were upregulated by stroke in mice on both diets, in general, the relative upregulation

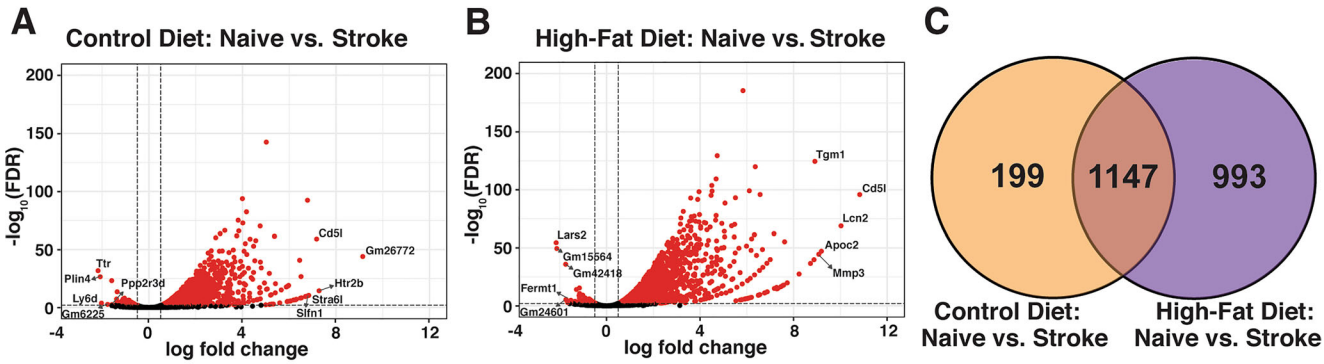

D

Control Diet Only (199 genes)

ID	GO Term	q-Value
55002	striated muscle cell development	8.55E-03
6941	striated muscle contraction	8.55E-03
8015	blood circulation	8.55E-03
3012	muscle system process	8.93E-03
7626	locomotory behavior	8.93E-03
6936	muscle contraction	8.93E-03
55001	muscle cell development	8.93E-03

Both Diets (1147 genes)

ID	GO Term	q-Value
98542	defense response to other organisms	7.22E-40
9617	response to bacterium	3.08E-31
50778	positive regulation of immune response	7.18E-30
45087	innate immune response	8.87E-29
50900	leukocyte migration	2.78E-27
2274	myeloid leukocyte activation	3.08E-25
2443	leukocyte mediated immunity	2.09E-24
9615	response to virus	5.57E-23
9897	external side of plasma membrane	1.72E-22
42742	defense response to bacterium	4.22E-22
31349	positive regulation of defense response	5.08E-22
51272	positive regulation of cellular component movement	4.21E-21
200047	positive regulation of cell motility	4.32E-21
30335	positive regulation of cell migration	6.66E-21
2697	regulation of immune effector process	2.33E-20
1819	positive regulation of cytokine production	2.33E-20
2253	activation of immune response	1.38E-19
32103	positive regulation of response to external stimulus	1.56E-19
45088	regulation of innate immune response	4.01E-19
2237	response to molecule of bacterial origin	1.20E-17

High Fat Diet Only (993 genes)

ID	GO Term	q-Value
48514	blood vessel morphogenesis	2.23E-07
30198	extracellular matrix organization	5.45E-06
43062	extracellular structure organization	5.45E-06
2460	adaptive immune response based on somatic recombination of immune receptors	1.48E-05
1667	ameboidal cell migration	4.51E-05
30199	collagen fibril organization	4.51E-05
9617	response to bacterium	5.63E-04
2250	adaptive immune response	7.39E-04
45765	regulation of angiogenesis	7.53E-04
10361	epithelial cell migration	8.16E-04
1901-342	regulation of vasculature development	8.44E-04
1570	vasculogenesis	1.05E-03
45087	innate immune response	1.79E-03
16684	oxidoreductae activity, acting on peroxidase as an acceptor	1.81E-03
4601	peroxidase activity	1.81E-03
31349	positive regulation of defense response	2.34E-03
2449	lymphocyte mediated immunity	2.59E-03
31012	extracellular matrix	3.15E-03
2237	response to molecule of bacterial origin	3.94E-03
35924	response to vascular endothelial growth factor stimulus	3.94E-03

Innate & general immune
Vasculogenesis / angiogenesis
Extracellular matrix/ tissue re-organization
Adaptive immune

Fig. 6 Differential gene expression in the cortex of naïve animals compared to 3 days after stroke in control and high-fat diet-fed animals. **a** Volcano plots indicating levels of differential gene expression in control animals both before (naïve) and 3 days after stroke. **b** Volcano plots indicating levels of differential gene expression in high-fat diet-fed animals both before (naïve) and 3 days after stroke. The log fold change in gene expression between pairs of conditions is plotted against the false discovery rate (FDR, in negative log base 10). Genes highlighted in red indicate significance at FDR < 0.01. **c** Venn diagram showing the number and overlap in genes significantly different between naïve and 3 days after stroke (FDR < 0.01), comparing control and high-fat diet. **d** Tables of top GO pathways altered in the gene sets upregulated by stroke in control diet–fed animals only (left), in both conditions (middle), and only in high-fat diet-fed animals (right). Pathways are color coded into four main biological effects: general and innate inflammation (yellow), vasculogenesis/angiogenesis (pink), extracellular matrix and tissue reorganization (purple), and adaptive immunity (blue)

by high-fat diet was higher for pro-inflammatory genes than for anti-inflammatory genes (Fig. 7b). To provide easily accessible data to stroke scientists interested in obesity, we designed a website that displays our transcriptomic data (buckwalterlab.shinyapps.io/SixWeekHighFatDietStrokeData/).

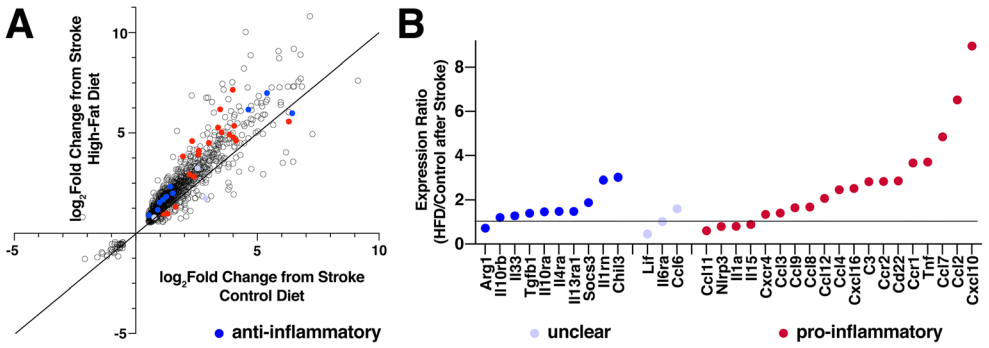

Fig. 7 Increased pro-inflammatory gene expression in the cortex 3 days after stroke in high-fat diet mice. All genes were significantly upregulated by stroke in both control diet and high-fat diet-fed animals (FDR < 0.01). Selected genes were colored according to their classical inflammatory roles. **a** Scatterplot of $\log_2$ fold change induced by stroke in control diet (*x*-axis) versus high-fat diet (*y*-axis). **b** Expression ratio (high-fat diet/control diet) of gene fold changes between diets 3 days after stroke

Discussion

In summary, we examined the effects of diet-induced obesity on stroke outcomes. We replicated other's results that high-fat diet induced larger strokes at 3 days accompanied by increases in neuroinflammation in diet paradigms lasting either 6 weeks or 15 weeks. After establishing this, we focused on the 6-week paradigm and described for the first time that this is due to increased infarct expansion between 10 hours and 3 days after stroke in obese mice. Increases in neuroinflammation also were not present prior to stroke and appeared after 10 hours, highlighting a potential therapeutic window after stroke. Finally, we report here the first transcriptome of obese stroke and describe molecular responses, and make the data publicly available on an easily accessed website for other researchers. We observed very few gene expression changes in the cortex prior to stroke. In addition to increased inflammatory gene expression at 3 days (buckwalterlab.shinyapps.io/SixWeekHighFatDietStrokeData/), obesity promoted genes related specifically to extracellular matrix generation, adaptive immune responses, and angiogenesis/vasculogenesis. Importantly, in our studies, all animals were fed a normal control diet after stroke to model standard patient care. Thus, the observed effects are due to the chronic influence of diet on neuroinflammation rather than an acute effect of high-fat diet after stroke.

Our observation of increased infarct expansion from obesity is novel; however, it is consistent with other reports of larger infarcts in high-fat diet-fed animals, measured at a single time point between 1 day and 1 week after stroke [24–26, 28, 30, 57–61]. In genetic animal models of obesity and diabetes, strokes are also typically larger, and inflammation has been implicated (reviewed in [32, 62, 63]) and related to leptin resistance [64], which we did not examine here. We were also able to demonstrate larger infarct size in two separate models of stroke, suggesting that this response is a physiologically relevant response.

We employed two animal models of stroke to assure these changes were not solely due to a consequence of using either a thrombotic or an ischemic model. We utilized the dMCAO model as a more clinically relevant model to measure neuroinflammation in the peri-infarct area as it portrays a very clear infarct border. While the dMCAO model creates infarcted tissue in the sensory cortices [37], it is difficult to test mice for sensory deficits. Additionally, sensory tests that have been used in the literature, like the adhesive removal task, and the corner test only demonstrate functional deficits for 1 day following surgery [65, 66] due to rapid spontaneous recovery. This time window does not allow enough time to measure the functional results of later infarct expansion. While the dMCAO model was the central focus of this study, the photothrombotic model over the motor cortex was utilized as a confirmatory experiment to measure functional deficits that were exacerbated in the high-fat diet-fed animals. The high-fat diet-fed animals had increased infarcts in both of these stroke models.

Several mechanisms may lead to larger infarcts in obesity and are likely related to infarct expansion that we report here. Infarcts could be larger in obese animals due to endothelial dysfunction and arterial stiffness, which are one of the initial effects of obesity [67–69]. This would be expected to cause strokes to be initially larger in models with a large penumbra [32], but in our dMCAO model, there is a limited penumbra and infarct size should be relatively resistant to stiffness-induced changes in collateral blood flow. Thus, its contribution to stroke size is likely dependent on the availability of collateral circulation, which was not a significant factor in our study. This allowed us to isolate the effects of obesity on neuroinflammation after stroke and learn more about this therapeutically accessible target. However, vascular dysfunction is likely an important contributory mechanism to stroke size in people with obesity and stroke.

Second, the peripheral inflammation caused by diet-induced obesity might lead to increased brain inflammation either prior to

or at the time of stroke. We performed careful analysis by qPCR, and RNA sequencing examined this in mice fed 6 weeks of high-fat diet and did not see increased brain inflammation, so increased cortical inflammation prior to stroke was not a factor in infarct expansion. Specifically, there was no upregulation of inflammatory genes in obese mice prior to stroke nor increases in microgliosis and astrogliosis or key inflammatory genes before and 10 hours after stroke. To our knowledge, others have not examined very early time points ≤ 10 hours after stroke in stroke and obesity studies. Since there is two-way communication between the brain and peripheral immune system following stroke, it is important to consider systemic inflammation [70, 71].

Although we did not see cortical neuroinflammation prior to stroke in obese mice, in other models and in some obese people, there is likely obesity-induced neuroinflammation that would amplify the effects we report here. Prior studies in diet-induced obesity models are conflicting. Some report an absence of cortical neuroinflammation [72–75] while others using longer diet regimens do find it [76, 77]. For example, male C57B6/J mice fed up to 4 months on high-fat diet had 1.5-fold increases in TNF, IL-6, and IL-1β in the cortex [76]. Studies on the hypothalamus, which has increased blood-brain barrier permeability [78], more consistently report obesity-induced neuroinflammation [18, 79–82]. We also used female mice here, which exhibit less hypothalamic inflammation in diet-induced obesity [22], and there are inter-model differences in diet composition, genetic background, and housing conditions that also may influence neuroinflammation.

Finally, the most likely cause in our model is obesity-induced systemic inflammation, where cells and/or inflammatory mediators gain access to the brain after the stroke and induce late neuroinflammation, after 10 hours [70, 71, 83]. The evidence for this is that we saw increased infarct expansion between 10 hours and 3 days in high-fat diet-fed mice and increased activation of astrocytes and microglia/macrophages during the same time period. Notably, at 10 hours, we did not see increased blood-brain barrier permeability (data not shown) or increases in cytokine expression in high-fat diet-fed mice compared to those on control diet. We counted peri-infarct Iba1-expressing cells and saw morphology consistent with increased activation but not increased cells in obese mice, implying that the increased neuroinflammation was related to increased activation of each cell rather than more cells invading the stroked brain. Indeed, hyper-activation of the peripheral immune system is well described in obesity [7–14], and in obese mice following stroke, there are increases in plasma free fatty acids, pro-inflammatory cytokines, and several membrane lipids which affect both the metabolism and inflammatory response following stroke and may lead to the worsened outcomes associated with stroke and obesity [83]. In the future, we may be able to target obesity-induced peripheral inflammation prior to its effects on neuroinflammation and infarct expansion.

Our RNA sequencing results from mice fed high-fat diet or control diet for 6 weeks brought out several interesting pathways that are altered by diet-induced obesity and are potential therapeutic targets. The innate inflammatory response to stroke was similar but amplified in the obese mice compared to those fed control diet, with almost all gene changes higher in the high-fat diet-fed animals. GO pathways were overwhelmingly related to innate inflammation and general immune responses, and although pro-inflammatory genes were slightly more upregulated than anti-inflammatory genes, there was not a clear signal of differential polarization of the immune response. This is distinct from obesity-induced inflammation in adipose tissue, where macrophages are polarized towards a more pro-inflammatory state [84–87]. Peripheral blood mononuclear cells are also more activated in obesity and demonstrate a propensity to excrete higher levels of pro-inflammatory cytokines after stimulation [88, 89]. Stroke itself also acts as a highly pro-inflammatory stimulus to peripheral immune cells [90] as well as in the cortex as we report here. So, the increased innate inflammation we see in obese animals after stroke is likely a result of synergy between the stimulus of obesity and that of stroke.

There were three biological processes that were altered by stroke in high-fat diet-fed but not control diet–fed animals. Each is implicated in the negative effects of obesity in other organs, and effects on stroke recovery remain unknown but are likely harmful. Extracellular matrix remodeling is implicated in obesity-induced insulin resistance [91] and contributes to higher cancer risk [92, 93]. In stroke, extracellular matrix differences could hinder normal axonal sprouting and rewiring during recovery [94, 95]. Increased adaptive inflammation in obese animals happens in adipose tissue [8, 9, 84, 87, 96]. In the brain after stroke, adaptive immune responses may increase both chronic inflammation and autoreactivity against brain antigens after stroke, both implicated in post-stroke cognitive impairment [97]. Finally, obesity altered angiogenic and vasculogenic pathways after stroke, and it is known to promote angiogenesis in adipose tissues [98], but conversely to impair wound healing by impairing vasculogenesis [99, 100]. Genes driving these GO pathways in our stroke model included endothelial receptors like Tek (Tie-2), Adgra2, Tie1, and Acvrl1, implying that obesity is altering brain endothelial cell gene expression after stroke. Notably, in obese animals, stroke did not increase Vegf expression, which is a strong driver of angiogenesis, plus there was a 2-fold upregulation of the angiogenesis inhibitor angiopoietin 2 (Angpt2). This may mean that the differences in these pathways result in less angiogenesis in obese animals after stroke.

It is important to consider that it is unlikely that all obesity-induced molecular changes are harmful, and some are likely

beneficial. Transthyretin was highly increased in high-fat diet-fed animals both before and after stroke and was downregulated by stroke in control diet–fed animals. However, deciphering its role is challenging. Transthyretin is a multifunctional pre-albumin that is named for its role in transporting thyroid hormone (T4) but also transports many other proteins [101]. One of these is retinol, or vitamin A, and both T4 and retinol are neuroprotective, so Ttr upregulation may be beneficial in stroke [102]. Indeed, Ttr has been directly implicated in neuroprotection in the setting of impaired heat shock responses [103]. Much less is known about the folate receptor Folr1, which is also prominently upregulated by high-fat diet. Its paralog Folr2 is a pro-resolution/M2 macrophage marker [104], so its upregulation may also be advantageous.

Some advantageous gene expression changes may explain the *obesity paradox*. The obesity paradox is that although obesity is a risk factor for many diseases, it can also confer some protection from the effects of those diseases. However, this has not been consistently observed in mouse stroke studies and in human studies; although there are some positive studies, there are also methodological concerns [105].

Despite the possibility of some benefit to obesity, the net effect of diet-induced obesity in our study was not only to promote infarct expansion but also to worsen outcomes after stroke. Animals fed high-fat diet for up to 4 weeks after stroke were more functionally impaired by stroke. This is also in agreement with the literature which has shown deficits in motor coordination, activity, and neurological function in high-fat diet-fed animals following ischemic insult [24, 25, 27, 57, 58].

There are several factors outside the scope of this study that will be interesting to study in the future. First, we only examined females and effects of high-fat diet may be different in males [22]. Second, mice fed a high-fat diet can acquire other comorbidities like those seen in humans which may play a role in the initiation, magnitude, or prolongation of the neuroinflammatory response. We replicated the established evidence of the development of pathogenic glucose intolerance in feeding paradigms similar to ours [106, 107]. In mice fed high-fat diet for 15 weeks, there is likely type 2 diabetes in conjunction with diet-induced obesity [106, 107]. Notably, we did not see differences between the 6- and 15-week diet paradigms in stroke size, microgliosis, or astrogliosis at 3 days.

Our data is highly relevant to human health. The encouraging finding that infarct expansion has not yet occurred at 10 h after stroke means that there may be an accessible therapeutic window after stroke in the obese where targeting of inflammatory mechanisms can reduce stroke morbidity and mortality. Our RNA sequencing data points to several inflammatory pathways likely to be upstream of infarct expansion that are consistent with prior literature on diet-induced obesity and peripheral inflammation in humans as well as in mice. Future animal studies targeting these pathways in multiple animal models of obesity and stroke have a high potential to lead to treatments for obese people who suffer a stroke.

Acknowledgments This work used the Genome Sequencing Service Center by Stanford Center for Genomics and Personalized Medicine Sequencing Center, supported by NIH S10OD020141.

Author Contribution Marion S. Buckwalter designed and performed the research, analyzed the data, and wrote the paper. Todd C. Peterson designed and performed the research, analyzed the data, and wrote the paper. Kendra J. Lechtenberg designed and performed the research and analyzed the data. Brian D. Piening designed and performed the research and analyzed the data. Tawaun A. Lucas designed and performed the research and analyzed the data. Eric Wei analyzed the data. Hassan Chaib analyzed the data. Alexa K. Dowdell analyzed the data. Michael Snyder designed the research and analyzed the data.

Funding Information This work was supported by the National Institute of Neurological Disorders and Stroke, RO1 NS067132 (Buckwalter) and NRSA F32 NS089162 (Peterson), and by a Brain Health Frontiers Award from the American Heart Association and the Paul Allen Frontiers Group. (Buckwalter)

Compliance with Ethical Standards

Competing Interests The authors declare that they have no competing interests.

Ethical Approval All applicable international, national, and/or institutional guidelines for the care and use for animals were followed. All use and care of animals was approved by UNCW IACUC protocol number A1819-01.

Informed Consent This article does not contain any studies with human participants performed by any of the authors.

References

1. Iadecola C, Anrather J. The immunology of stroke: from mechanisms to translation. Nat Med. 2011;17:796–808.
2. Heiss WD. The ischemic penumbra: how does tissue injury evolve? Ann N Y Acad Sci. 2012;1268:26–34.
3. Cekanaviciute E, Fathali N, Doyle KD, Williams AM, Han J, Buckwalter MS. Astrocytic transformating growth factor-beta signaling reduces subacute neuroinflammation after stroke in mice. Glia. 2014;62(8):1227–40.
4. Xu H. Obesity and metabolic inflammation. Drug Discov Today. 2013;10(1–2):21–5.
5. N. I. o. H. U.S. Department of Health and Human services, National Institute of Diabetes and Digestive and Kidney Diseases, Overweight & obesity statistics, Retrieved from https://www.niddk.nih.gov/health-information/health-statistics/overweight-obesity, 2010.
6. Strazullo P, D'Elia L, Cairella G, Garbagnati F, Cappuccio FP, Scalfi L. Excess body weight and incidence of stroke: meta-analysis of prospective studies with 2 million participants. Stroke. 2010;41(5):418–26.
7. Li P, Lu M, Nguyen MTA, Bae EJ, Chapman J, Feng D, et al. Functional heterogeneity of CD11c-positive adipose tissue macrophages in diet-induced obese mice. J Biol Chem. 2010;285(20):15333–45.

8. Lumeng CN, Bodzin JL, Saltiel AR. Obesity induces a phenotypic switch in adipose tissue macrophage polarization. J Clin Invest. 2007;117(1):175–84.
9. Lumeng CN, DelProposto J, Westcott DJ, Saltiel AR. Phenotypic switching of adipose tissue macrophages with obesity is generated by spatiotemporal differences in macrophage subtypes. Diabetes. 2008;57(12):3239–46.
10. Weissberg SP, McCann D, Desai M, Rosenbaum M, Leibel RL, Ferrante JW. Obesity is associated with macrophage accumulation in adipose tissue. J Clin Invest. 2003;112(12):1796–808.
11. Galvez I, Martin-Cordero L, Hinchado MD, Alvarez-Barrientos A, Ortega E. Anti-inflammatory effect of β2 adrenergic stimulation on circulating monocytes with a pro-inflammatory state in high-fat diet-induced obesity. Brain Behav Immun. 2019;19:30169–72.
12. Wisse B. The inflammatory syndrome: the role of adipose tissue cytokines in metabolic disorders linked to obesity. JASN. 2004;15(11):2792–800.
13. Greenberg AS, Obin MS. Obesity and the role of adipose tissue in inflammation and metabolism. Am J Clin Nutr. 2006;83(2):4615–55.
14. Coelho M, Oliveira T, Fernanes R. Biochemistry of adipose tissue: an endocrine organ. Arch Med Sci. 2013;9(2):191–200.
15. Pepping JK, Freeman LR, Gupta S, Keller JN, Bruce-Keller AJ. NOX2 deficiency attenuates markers of adiposopathy and brain injury induced by high-fat diet. Am J Physiol Endocrinol Metab. 2013;304:E392–404.
16. Takechi R, Pallebage-Gamarallage MM, Giles C, Mamo JC. Nutraceutical agents with anti-inflammatory properties prevent dietary saturated-fat induced disturbances in blood-brain barrier function in wild-type mice. J Neuroinflammation. 2013;19(10):73–85.
17. Costa de Aquino C, et al. Effect of hypoproteic and high-fat diets on hippocampal blood-brain barrier permeability and oxidative stress. Front Nutr. 2018;5:131–41.
18. Valdearcose M, et al. Microglial inflammatory signal orchestrates he hypothalamic immune response to dietary excess and mediates obesity susceptibility. Cell Metab. 2017;26:185–97.
19. Buckman LB, Thompson MM, Moreno HN, Ellacot KL. Regional astrogliosis in the mouse hypothalamus in response to obesity. J Comp Neurol. 2013;521:322–33.
20. Noronha SSR, et al. Association of high-fat diet with neuroinflammation, anxiety-like defensive behavioral responses, and altered thermoregulatory responses in male rats. Brain Behav Immun. 2019;19:30137–10349.
21. Rahman MH, Kim MS, Lee IK, Yu R, Suk K. Interglial crosstalk in obesity-induced hypothalamic inflammation. Front Neurosci. 2018;13(12):939–48.
22. Lainez NM, et al. Diet-induced obesity elicits macrophage infiltration and reduction in spine density in the hypothalami of male but not female mice. Front Immunol. 2018;11(9):1992–2008.
23. Lee CH, Kim HJ, Lee YS, Kang GM, Lim HS, Lee SH, et al. Hypothalamic macrophage inducible nitric oxide synthase mediates obesity-associated hypothalamic inflammation. Cell Rep. 2018;25(4):934–46.
24. Wu M, et al. Obesity exacerbates rat cerebral ischemic injury through enhancing ischemic adiponectin-containing neuronal apoptosis. Mol Neurobiol. 2016;53:3702–13.
25. Yang Z, Chen Y, Zhang Y, Yiang Y, Fang X, Xu J. Sevoflurane postconditioning against cerebral ischemic neuronal injury is abolished in diet-induced obesity: role of brain mitochondrial KATP channels. Mol Med Rep. 2014;8:843–50.
26. Deutsch C, Portik-Dobos D, Smith AD, Ergul A, Dorrance AM. Diet-induced obesity causes cerebral vessel remodeling and increase the damage cause by ischemic stroke. Microvasc Res. 2009;78:100–6.
27. Yan BC, Park JH, Ahn JH, Kim IH, Lee JC, Yoo KY, et al. Effects of high-fat diet on neuronal damage, gliosis, inflammatory process, and oxidative stress in the hippocampus induced by transient cerebral ischemia. Neurochem Res. 2014;39(12):2465–78.
28. Cao X, Du Y, Yan J, Hu X. Hyperlipidemia exacerbates cerebral injury through oxidative stress, inflammation, and neuronal apoptosis in MCAO/reperfusion rats. Exp Brain Res. 2015;233:2753–65.
29. Kim E, Yang J, Park KW, Cho S. Inhibition of VEGF signaling reduces diabetes-exacerbated brain swelling, but not infarct size, in large cerebral infarction in mice. Transl Stroke Res. 2018;9(5):540–8.
30. Haley MJ, Krishnan S, Burrows D, de Hoog L, Thakrar J, Schiessl I, et al. Acute high-fat feeding leads to disruptions in glucose homeostasis and worsens stroke outcome. J Cereb Blood Flow Metab. 2019;39(6):1026–37.
31. Kim E, Yang J, Woo Park K, Cho S. Preventative, but not post-stroke, inhibition of CD36 attenuates brain swelling in hyperlipidemic stroke. J Cereb Blood Flow Metab. 2019;15:1–8.
32. McColl BW, Rose N, Robson FH, Rothwell NJ, Lawrence CB. Increased brain microvascular MMP-9 and incidence of haemorrhagic transformation in obese mice after experimental stroke. J Cereb Blood Flow Metab. 2010;30(2):267–72.
33. Maysami S, Haley MJ, Gorenkova N, Krishnan B, McColl BW, Lawrence CB. Prolonged diet-induced obesity in mice modifies the inflammatory response and leads to worsened outcomes after stroke. J Neuroinflammation. 2015;12:140–52.
34. King VL, Hatch NW, Chan HW. A murine model of obesity with accelerated athersclerosis. Obesity. 2009;18(1):35–41.
35. Y. Hang et al., The MafA transcription factor becomes essential to islet β-cells soon after birth, Diabetes, p. DB_131001, 2014.
36. Tamura A, Graham DI, McCulloch J, Teasdale GM. Focal cerebral ischemia in the rat: description of technique and early pathological consequences following middle cerebal artery occlusion. J Cereb Blood Flow Metab. 1981;1:53–60.
37. Doyle KP, Fathali N, Siddiqui AM, Buckwalter BL. Distal hypoxic stroke: a new mouse model of stroke with high throughput, low variability, and a quantifiable functional deficit. J Neurosci Methods. 2012;207:31–40.
38. Nouraee C, Fisher M, di Napoli M, Salazar P, Farr TD, Jafarli A, et al. A brief review of edema-adjusted infarct volume measurement techniques for rodent focal cerebral ischemia models with practical recommendations. Journal of Vascular and Interventional Neurology. 2019;10:38–45.
39. Schaar KL, Brenneman MM, Savitz SI. Functional assessments in the rodent stroke model. Exp Transl Stroke Med. 2010;2:13–24.
40. Shah AM, et al. Optogenetic neuronal stimulation of the lateral cerebellar nucleus promotes persistent functional recovery after stroke. Sci Rep. 2017;1(7):1–11.
41. Cheng MY, Aswendt M, Steinberg GK. Optogentic approaches to target specific neural circuits in post-stroke recovery. Neurotherapeutics. 2016;13(2):325–40.
42. Cheng MY, et al. Optogenetic neuronal stimulation promotes functional recovery after stroke. Proc Natl Acad Sci U S A. 2014;2(111):12913–8.
43. Wang J, Lin X, Mu Z, Shen F, Zhang L, Xie Q, et al. Rapamycin increases collateral circulation in rodent brain after focal ischemia as detected by multiple modality dynamic imaging. Theranostics. 2019;9(17):4923–34.
44. M. D. Robinson, D. J. McCarthy, and G. K. Smyth, edgeR: a bioconductor package for differential expression analysis of digital gene expression data, Bioinformatics, vol. 26, no. 1, pp. 139–140, 2010.
45. McCarthy DJ, Chen Y, Smyth GK. Differential expression analysis of multifactor RNA-Seq experiments with respect to

biological variation. Nucleic Acids Res. 2012;40(10):4288–97. https://doi.org/10.1093/nar/gks042.
46. Shannon P, Markiel A, Ozier O, Baliga NS, Wang JT, Ramage D, et al. Cytoscape: a software environment for integrated models of biomolecular interaction networks. Genome Res. 2003;13(11): 2498–504.
47. Warde-Farley D, Donaldson SL, Comes O, Zuberi K, Badrawi R, Chao P, et al. The GeneMANIA prediction server: biological network integration for gene prioritization and predicting gene function. Nucleic Acids Res. 2010;38:W214–20.
48. Love MI, Huber W, Anders S. Moderated estimation of fold change and dispersion for RNA-seq data with DESeq2. Genome Biol. 2014;15:550–71.
49. R. C. Team, R: a language and environment for statistical computing. R Foundational Computing, Vienna, Austria, 2013. [Online]. Available: http://www.R-project.org/.
50. Bates D, Machler M, Bolker BM, Walker SC. Fitting linear mixed-effects models using lme4. J Stat Softw. 2015;67(1):1–48.
51. Young ME, Clark MH, Goffus A, Hoane MR. Mixed effects modeling of Morris water maze data: advantages and cautionary notes. Learn Motiv. 2008;40:160–77.
52. Zeng H, Vaka VR, He X, Booz GW, Chen J. High-fat diet induces cardiac remodeling and dysfunction: assessment of the role played by SIRT3 loss. J Cell Mol Med. 2015;19(8):1847–56.
53. Ono-Moore KD, Ferguson M, Blackburn ML, Issafras H, Adams SH. Application of an in vivo hepatic triacylglycerol production method in the setting of a high-fat diet in mice. Nutrients. 2016;9: 1–16.
54. M. Cao et al., Adipose-derived mesenchymal stem cells improve glucose homeostasis in high-fat diet-induced obese mice, Stem Cell Research & Therapy, vol. 6, no. 1, p. 208, 2015.
55. L. M. Williams et al., The development of diet-induced obesity and glucose intolerance in C57BL/6 mice on a high-fat diet consists of distinct phases, PLoS One, vol. 9, no. 8, p. e106159, 2014.
56. K. L. Lechtenberg, S. T. Meyer, J. B. Doyle, T. C. Peterson, and M. S. Buckwalter, Augmented beta2-adrenergic signaling dampens the neuroinflamatory response following ischemic stroke and increases stroke size, Journal of Neuroinflammation, vol. 16, no. 112–130, 2019.
57. Deng J, Zhang J, Feng C, Xiong L, Zuo Z. Critical role of matrix metalloprotease-9 in chronic high-fat diet induced cerebral vascular remodelling and increase ischaemic brain injury in mice. Cardiovasc Res. 2014;103:473–84.
58. Li W, Prakash R, Chawla D, du W, Didion SP, Filosa JA, et al. Early effects of high-fat diet on neurovascular function and focal ischemic brain injury. Am J Physiol Integr Comp Physiol. 2013;304:R1001–8.
59. Dhungana H, et al. Western-type diet modulates inflammatory response and impairs functional outcome following permanent middle cerebral artery occlusion in aged mice expressing the human apolipoprotein E4 allele. J Neuroinflammation. 2013;10: 102–15.
60. Kim E, Tolhurst AT, Qin LY, Chen X, Febbraio M, Cho S. CD36/fatty acid translocase, an inflammatory mediator, in involved in hyperlipidemia-induced exacerbation in ischemic brain injury. J Neurosci. 2008;28(18):4661–7670.
61. Kim E, Yang J, Woo Park K, Cho S. Preventative, but not post-stroke, inhibition of CD36 attenuates brain swelling in hyperlipidemic stroke. J Cereb Blood Flow Metab. 2019;15:1–10.
62. Haley MJ, Lawrence CB. Obesity and stroke: can we translate from rodents to patients? J Cereb Blood Flow Metab. 2016;36(12):2007–21.
63. Kim E, Tolhurst AT, Cho S. Deregulation of inflammatory response in the diabetic condition is associated with increased ischemic brain injury. J Neuroinflammation. 2014;1(11):1–9.
64. Saiinz N, Barrenetxe J, Moreno-Aliagra MJ, Martinez JA. Leptin resistance and diet-induced obesity: central and peripheral actions of leptin. Metabolism. 2015;64(1):35–46.
65. Lubjuhn J, Gastens A, von Wilpert G, Bargiotas P, Herrmann O, Murikinati S, et al. Functional testing in a mouse stroke model induced by occlusion of the distal middle cerebral artery. J Neurosci Methods. 2009;184(1):95–103.
66. F. Luo et al., Cuprizone-induced demyelination under physiological and post-stroke condition leads to decreased neurogenesis response in adult mouse brain. Exp Neurol, vol. 326, 2020.
67. Calvalcante JL, Lima JA, Redheuil A, Al-Mallah MH. Aortic stiffness: current understanding and future directions. J Am Coll Cardiol. 2011;57(14):1511–22.
68. Stenmark KR, Yeager ME, el Kasmi KC, Nozik-Grayck E, Gerasimovskaya EV, Li M, et al. The adventitia: essential regulator of vascular wall structure and function. Annu Rev Physiol. 2013;75:23–47.
69. Muniyappa R, Sowers JR. Role of insulin resistance in endothelial dysfunction. Rev Endocr Metab Disord. 2013;14(1):5–12.
70. Kim E, Cho S. Microglia and monocyte-derived macrophages in stroke. Neurotherapeutics. 2016;13(4):702–18.
71. C. J. Smith, C. B. Lawrence, B. Rodrguez-Grande, K. J. Kovacs, J. M. Pradillo, and A. Denes, The immune system in stroke: clinical challenges and their translation to experimental research, J Neuroimmune Pharmacol, vol. 8, no. 867–887, 4, 2013.
72. Pistell PJ, Morrison CD, Gupta S, Knight AG, Keller JN, Ingram DK, et al. Cognitive impairment following high fat diet consumption is associated with brain inflammation. J Neuroimmunol. 2010;219:25–32.
73. Guillemot-Legris O, Masquelier J, Everard A, Cani PD, Alhouayek M, Muccioli GG. High-fat diet feeding differentially affects the development of inflammation in the central nervous system. J Neuroinflammation. 2016;13(1):206–17.
74. Wang S, Huang XF, Zhang P, Wang H, Zhang Q, Yu S, et al. Chronic rhein treatment improves recognition memory in high-fat diet-induced obese male mice. J Nutr Biochem. 2016;36:42–50.
75. Tarantini S, et al. Nrf2 deficiency exacerbates obesity-induced oxidative stress, neurovascular dysfunction, blood–brain barrier disruption, neuroinflammation, amyloidogenic gene expression, and cognitive decline in mice, mimicking the aging phenotype. J Gerontol A Biol Sci Med Sci. 2017;73(7):853–63.
76. Jayaraman A, Lent-Schochet D, Pike CJ. Diet-induced obesity and low testosterone increase neuroinflammation and impair neural function. J Neuroinflammation. 2014;11:162–76.
77. J. L. Carlin, N. Grissom, Z. Ying, F. Gomez-Pinilla, and T. M. Reyes, Voluntary exercise blocks Western diet-induced gene expression of the chemokines CXCL10 and CCL2 in the prefrontal cortex. Brain Behav Immun, vol. 58, no. 82–90, 2016.
78. Rodriguez EM, Blazquez JL, Guerra M. The design of barriers in the hypothalamus allows the median eminence and the arcuate nucleus to enjoy private millieus: the former opens to the portal blood and the latter to the cerebral spinal fluid. Peptides. 2010;31(4):757–76.
79. S. Kalin, F. L. Heppner, I. Bechmann, M. Prinz, M. H. Tschop, and C. Yi, Hypothalamic innate immune reaction in obesity, Nature Reviews Endocrinology, vol. 11, no. 339–351, 2015.
80. Zhang X, Zhang G, Zhang H, Karin M, Bai H, Cai D. Hypothalamic IKKB/NfkB and ER stress link overnutrition to energy imbalance and obesity. Cell. 2008;135(1):61–73.
81. Waise TM, et al. One-day high-fat diet induced inflammation in the nodose ganglion and the hypothalamus. Biochem Biophys Res Commun. 2015;464(4):1157–62.
82. Thaler JP, Yi CX, Schur EA, Guyenet SJ, Hwang BH, Dietrich MO, et al. Obesity is associated with hypothalamic injury in rodents and humans. J Clin Invest. 2012;122(1):153–62.

83. Haley MJ, Mullard G, Hollywood KA, Cooper GJ, Dunn WB, Lawrence CB. Adipose tissue and metabolic and inflammatory responses to stroke are altered in obese mice. Dis Model Mech. 2017;10(10):1229–43.
84. Morris DL, Cho KW, DelProposto JL, Oatmen KE, Geletka LM, Martinez-Santibanez G, et al. Adipose tissue macrophages function as antigen-presenting cells and regulated adipose tissue CD4+ cells in mice. Diabetes. 2013;62:2762–72.
85. Surmi BK, Hasty AH. Macrophage infiltration into adipose tissue: initiation, propogation, and remodeling. Future Lipidol. 2008;3(5):545–56.
86. Zheng C, et al. CD11b regulates obesity-induced insulin resistence via limiting alternative activation and proliferation of adipose tissue macrophages. Proc Natl Acad Sci U S A. 2015;111(52):7239–48.
87. Cho KW, et al. An MHC II-dependent activation loop between adipose tissue macrophages and CD4+ T cells controls obesity induced inflammation. Cell Rep. 2009;9:605–17.
88. D. Dicker, M. A. Salook, D. Marcoviciu, M. Djaldetti, and H. Bessler, Role of peripheral blood mononuclear cells in the predisposition of obese individuals to inflammation and infection, Obesity Facts, vol. 6, no. 146–151, 2013.
89. Catalan V, et al. Peripheral mononuclear blood cells contribute to the obesity-associated inflammatory state independently of glycemic status: involvement of the novel proinflammatory adipokines chemerin, chitinase-3-like protein 1, lipocalin-2 and osteopontin. Genes and Nutrition. 2015;10(11):1–11.
90. Tsai AS, Berry K, Beneyto MM, Gaudilliere D, Ganio EA, Culos A, et al. A year-long immune profile of the systemic response in acute stroke survivors. Brain. 2019;142(4):978–91.
91. Williams AS, Kang L, Wasserman DH. The extracellular matrix and insulin resistance. Trends Endocrinol Metab. 2015;26(7):357–66.
92. Seo BR, et al. Obesity-dependent changes in interstitial ECM mechanics promote breast tumorigenesis. Sci Transl Med. 2015;19(7):1–11.
93. Quail DF, Dannenberg AJ. The obese adipose tissue microenvironment in cancer development and progression. Nat Rev Endocrinol. 2019;15(3):139–54.
94. Dzyubenko E, Manrique-Castano D, Kleinschnitz C, Faissner A, Hermann DM. Role of immune responses for extracellular matrix remodeling in the ischemic brain. Ther Adv Neurol Disord. 2018;11:1–11.
95. Oliveira Dias D, Gortiz C. Fibrotic scarring following lesions to the central nervous system. Matrix Biol. 2018;68-69:561–70.
96. Deng T, et al. Class II major histocompatibility complex plays an essential role in obesity-induced adipose inflammation. Cell Metab. 2013;5(17):411–22.
97. Doyle KP, Buckwalter BL. Does B lymphocyte-mediated autoimmunity contribute to post-stroke dementia? Brain Behav Immun. 2017;64:1–8.
98. Cao Y. Angiogenesis modulates adipogenesis and obesity. J Clin Invest. 2007;117(9):2362–8.
99. Wagner IJ, et al. Obesity impairs wound closure through a vasculogenic mechanism. Wound Repair Regen. 2012;20(4):512–22.
100. M. J. Haley et al., Stroke induces prolonged changes in lipid metabolism, the liver, and body composition in mice, Translational Stroke Research, pp. 1–14, 2019, doi: https://doi.org/10.1007/s12975-019-00763-2.
101. Liz MA, Mar FM, Franquinho F, Sousa M. Aboard transthyretin: from transport to cleavage. Life. 2010;62(6):429–35.
102. Lin HY, et al. Molecular basis for certain neuroprotective effects of thyroid hormone. Front Mol Neurosci. 2011;14(4):1–6.
103. Santos SD, Lambertsen KL, Clausen BH, Akinc A, Alvarez R, Finsen B, et al. CSF transthyretin neuroprotection in a mouse model of brain ischemia. J Neurochem. 2010;115:1434–44.
104. Puig-Kroger A, Sierra-Filardi E, Dominguez-Soto A, Samaniego R, Corcuera MT, Gomez-Aguado F, et al. Folate receptor β is expressed by tumor-associated macrophages and constitutes a marker for M2 anti-inflammatory/regulatory macrophages. Cancer Res. 2009;69(24):9395–403.
105. L. Oesch, T. Tatlisumak, M. Arnold, and H. Sarikaya, Obesity paradox in stroke - myth or reality? A systematic review. PLoS One, vol. 12, no. 3, p. e0171334, 2017.
106. Mosser RE, Maulis MF, Moullé VS, Dunn JC, Carboneau BA, Arasi K, et al. High-fat diet-induced β-cell proliferation occurs prior to insulin resistance in C57Bl/6J male mice. Endocrinol Metab. 2015;308(7):E573–82.
107. Heydemann A. An overview of murine high fat diet as a model for type 2 diabetes mellitus. Journal of Diabetes Research. 2016;2016:1–14.